

NT@UW-00-30

Trouble in Asymptopia—the Hulthén Model on the Light Front

B. C. Tiburzi and G. A. Miller

Department of Physics
 University of Washington
 Box 351560
 Seattle, WA 98195 – 1560

January 30, 2020

Abstract

We use light-front dynamics to calculate the electromagnetic form-factor for the Hulthén model of the deuteron. For small momentum transfer $Q^2 < 5 \text{ GeV}^2$ the relativistic effects are quite small. For $Q^2 \sim 11 \text{ GeV}^2$ there is $\sim 13\%$ discrepancy between the relativistic and non-relativistic approaches. For asymptotically large momentum transfer, however, the light-front form factor, $\sim \log Q^2/Q^4$, markedly differs from the non-relativistic version, $\sim 1/Q^4$. This behavior is also present for any wave function, such as those obtained from realistic potential models, which can be represented as a sum of Yukawa functions. Furthermore, the asymptotic behavior is in disagreement with the Drell-Yan-West relation. We investigate precisely how to determine the asymptotic behavior and confront the problem underlying troublesome form factors on the light front.

1 Introduction

The light front approach to quantum dynamics was introduced by Dirac [1] a half century ago. Since then, light front dynamics has developed into an active area of research for a variety of reasons, e.g. its minimal set of dynamical operators, the simplicity of the light-front vacuum, and the close connection to experimental observables. Light front techniques have long been used in analyzing high energy experiments with nuclear and nucleon targets [2, 3, 4, 5]. Indeed light front dynamics is relevant to describe such reactions, since, for example: in the parton model, the ratio k^+ / p^+ (where $k^+ = k^0 + k^3$ is the plus momentum of the struck quark and p^+ that of the target) is nothing more than the Bjorken x -variable.

Some recent efforts have been made [6] to render the theory more understandable by using models reminiscent of basic quantum mechanics rather than by invoking quantum field theory. These models find particular reality in nuclear physics [7], where some nucleon interactions may be described by a mean field potential. Nonetheless, the similarity of the light-front bound state equation to the Schrödinger equation is grounds enough to put familiar quantum mechanical problems on the light front. Below, we do precisely this for the Hulthén model of the deuteron and its electromagnetic form factor. Of particular concern here is the asymptotic behavior of the form factor, which differs from the non-relativistic version. This may be of interest to experimentalists seeking to probe asymptopia. Recent measurements of deuteron form factors at the Jefferson National Laboratory [8] reach momentum transfers of $Q^2 = 6 \text{ GeV}^2$ and future projects hope to reach upwards of $Q^2 = 11 \text{ GeV}^2$. In this range of momentum transfer,

there is $\sim 13\%$ discrepancy between the relativistic and non-relativistic form factors calculated in this paper (as we will illustrate in figure 3).

This paper's organization is similar to that of a detective story. First we recall a minimal amount of light front dynamics in section 2 and explain how we put the non-relativistic Hulthén potential on the light front. Next in section 3, we calculate the electromagnetic form factor using light front dynamics and compare with the non-relativistic version calculated in section 4. The low momentum behavior of the these form factors shows only minimal differences, while the high momentum behavior leads to surprising trouble in asymptopia (section 5). We could solve the mystery at this point by deriving the asymptotic behavior of the form factor. Instead, we proceed by assuming factorization holds in the asymptotic limit. This leads us to consider various previous attempts at dealing with the end-point region and to dispel any lingering misconceptions. In section 6, we discover that troublesome asymptotic behavior also lurks in other models on the light front. With enough clues at hand, we are able to pin-point the cause. The asymptotic behavior is then deduced in section 7, and is similar to that obtained for the Wick-Cutkosky model in Ref. [9]. Finally, we summarize our findings in a brief concluding section.

2 Hulthén model on the light front

In light front dynamics, one quantizes the fields at equal light-front time specified by $x^+ = x^0 + x^3 = t + z$. This redefinition of the time variable leaves us with a new spatial variable $x^- = x^0 - x^3 = t - z$. The remaining spatial variables are left unchanged by this transformation: $\mathbf{x}^\perp = (x^1, x^2)$.

If one uses x^- as a spatial variable, then its momentum conjugate is $p^+ = p^0 + p^3$. This leaves $p^- = p^0 - p^3$ as the energy, or the x^+ -development operator. The details of this formalism do not concern us here—the interested reader should consult [10] for a good overview. What is important to note, however, is that the relativistic dispersion relation $p^\mu p_\mu = m^2$ takes the form

$$p^- = \frac{\mathbf{p}^\perp{}^2 + m^2}{p^+}, \quad (1)$$

and thus the expression for the kinetic energy avoids the historically problematic square root.

For a bound state of two particles interacting via a potential V , the light-front wave function is determined by solving the equation [11]

$$\psi = \frac{1}{M^2 - \sum_{i=1,2} \frac{k_i^\perp{}^2 + m_i^2}{x_i}} V \psi, \quad (2)$$

where M is the invariant mass of the system, m_i the particle mass, and x_i is the plus momentum fraction carried by the i^{th} particle, namely $x_i = k_i^+ / P^+$, with P^+ as the total plus momentum, $k_1^+ + k_2^+$. Let us take the nucleons to be of equal mass, and use $m = \frac{m_p + m_n}{2}$ as the nucleon mass. Furthermore, since we have only two particles, the sum of x_1 and x_2 is one. So we choose $x_1 \equiv x$ and consequently, $x_2 = 1 - x$.

In order to simplify Eq. 2, it is customary to define the relative light-front variables [12]

$$\begin{aligned} \mathbf{P}^\perp &= \mathbf{k}_1^\perp + \mathbf{k}_2^\perp \\ \mathbf{p}^\perp &= -x \mathbf{k}_1^\perp + (1 - x) \mathbf{k}_2^\perp. \end{aligned} \quad (3)$$

Straightforward algebra transforms Eq. 2 into

$$M^2 \psi = \left(\frac{\mathbf{p}^\perp{}^2 + m^2}{x(1-x)} + V \right) \psi, \quad (4)$$

which is the coordinate representation of the Weinberg equation [13]. Eq. 4 is still quite complicated to solve, so we define an auxiliary operator

$$p^3 = \left(x - \frac{1}{2}\right) \sqrt{\frac{\mathbf{p}^\perp{}^2 + m^2}{x(1-x)}} \quad (5)$$

to cast the equation into a familiar form. Defining $M = 2m - \epsilon$ (where ϵ is the binding energy) and using the above definition, we find

$$\begin{aligned} \left(\frac{\epsilon^2}{4} - \epsilon m\right)\psi &= \left(\mathbf{p}^\perp{}^2 + (p^3)^2 + \frac{V}{4}\right)\psi \\ &\equiv (\mathbf{p}^2 + V^H)\psi, \end{aligned} \quad (6)$$

where we have efficaciously chosen $V^H = V/4$ to be the Hulthén potential [14].

The above equation is the coordinate-space version considered by others, see e.g. [15]. Taking \mathbf{p} conjugate to \mathbf{r} , we have

$$V^H(\mathbf{r}) = \frac{b^2 - a^2}{1 - e^{(b-a)r}}, \quad (7)$$

and the well known ground state solution

$$\psi(r) \propto \frac{e^{-ar} - e^{-br}}{r} \quad (8)$$

with $a = \sqrt{\epsilon m - \epsilon^2/4}$ as dictated by Eq. 6. The experimentally determined values of the model parameters are [16]: $a = 0.23161 \text{ fm}^{-1}$ and $b = 1.3802 \text{ fm}^{-1}$.

3 Electromagnetic Form Factor

The electromagnetic form factor on the light front has the form [17]

$$F(Q^2) = \int \frac{dx d\mathbf{p}^\perp}{x(1-x)} \psi^*(x, \mathbf{p}^\perp + (1-x)\mathbf{q}^\perp) \psi(x, \mathbf{p}^\perp), \quad (9)$$

where the momentum transfer $Q^2 = \mathbf{q}^\perp{}^2$. The momentum-space Hulthén wave function is the Fourier transform of our solution Eq. 8, namely

$$\begin{aligned} \psi(x, \mathbf{p}^\perp) &\equiv \frac{m\sqrt{N}}{4} \left(\frac{1}{a^2 + \mathbf{p}^\perp{}^2 + (p^3)^2} - \frac{1}{b^2 + \mathbf{p}^\perp{}^2 + (p^3)^2} \right) \\ &= \frac{m\sqrt{N}x(1-x)}{4x(1-x)a^2 + (2x-1)^2m^2 + \mathbf{p}^\perp{}^2} \left(\delta_a^\alpha - \delta_b^\alpha \right). \end{aligned} \quad (10)$$

To calculate the form factor, we must perform three integrals. Writing $d\mathbf{p}^\perp = \mathbf{p}^\perp d\mathbf{p}^\perp d\phi$ with ϕ as the angle between \mathbf{p}^\perp and \mathbf{q}^\perp , we see the ϕ integral and subsequently the \mathbf{p}^\perp integral can be computed analytically. Performing these integrals leaves us with

$$F(Q^2) = \int_0^1 f(x, (1-x)^2 Q^2) dx, \quad (11)$$

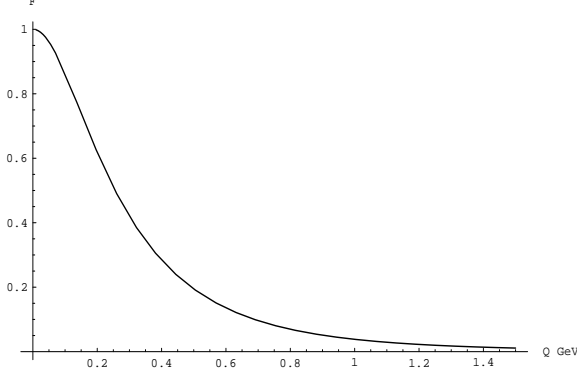


Figure 1: Plot of the light front Hulthén form factor Eq. 11 as a function of Q in GeV.

where

$$f(x, k^2) = m^2 N x (1 - x) g_{\alpha\beta}(x, k^2) \left(\delta_a^\alpha \delta_a^\beta - \delta_a^\alpha \delta_b^\beta - \delta_b^\alpha \delta_a^\beta + \delta_b^\alpha \delta_b^\beta \right) \quad (12)$$

with

$$g_{\alpha\beta}(x, k^2) = \frac{\pi}{\rho_{\alpha\beta}(x, k^2)} \log \left[\frac{k^4 + k^2(2\gamma_\alpha(x) + \gamma_\beta(x) + \rho_{\alpha\beta}(x, k^2)) + \gamma_\beta(x)(\rho_{\alpha\beta}(x, k^2) - \gamma_\beta(x) - \gamma_\alpha(x))}{\gamma_\alpha(x)(-k^2 + \rho_{\alpha\beta}(x, k^2) + \gamma_\beta(x) - \gamma_\alpha(x))} \right]$$

where we have defined

$$\begin{aligned} \gamma_\mu(x) &\equiv 4x(1-x)\mu^2 + (2x-1)^2 m^2 \\ \rho_{\alpha\beta}(x, k^2) &\equiv \sqrt{k^4 + 2k^2\gamma_\beta(x) + \gamma_\alpha(x)^2}. \end{aligned}$$

We choose N so that the form factor is normalized, $F(0) = 1$. The constant N is determined by setting $Q = 0$ in Eq. 9, which yields $N = 14.931^{-1}$. Figure 1 shows the form factor as a function of Q . We have also calculated the derivative of $F(Q^2)$ in the limit $Q \rightarrow 0$ in order to find the root-mean-square deuteron radius

$$R_{rms} = \lim_{Q^2 \rightarrow 0} \sqrt{-6 \frac{dF}{dQ^2}} = 1.9467 \text{ fm.} \quad (13)$$

4 The Non-Relativistic Limit and Comparison

Our solution to the Hulthén model on the light front closely resembles the non-relativistic treatment. In fact, we have used the non-relativistic solution as a guide in constructing the relativistic wave function. Clearly relativistic effects are contained in the light-front variable x . Quite simply then, the non-relativistic limit of Eq. 9 is found in the limit $m \rightarrow \infty$ by retaining terms to $\mathcal{O}[\frac{1}{m}]$. Inverting Eq. 5 yields

$$x = \frac{1}{2} + \frac{p^3}{2\sqrt{\mathbf{p}^{\perp 2} + (p^3)^2 + m^2}} \approx \frac{1}{2} + \frac{p^3}{2m}. \quad (14)$$

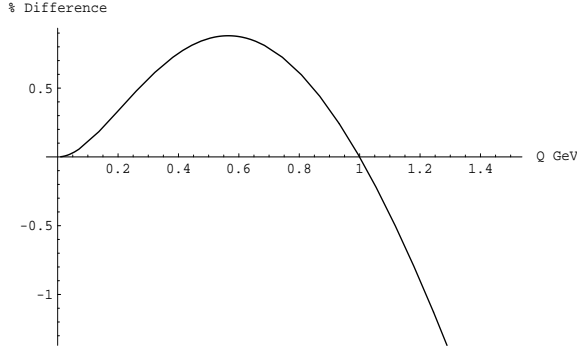


Figure 2: Relativistic and non-relativistic form factor comparison: percent difference: $100 \times (F^{\text{NR}} - F)/F^{\text{NR}}$ plotted as a function of Q in GeV.

Since the measure $dx \, d\mathbf{p}^\perp \rightarrow d\mathbf{p}/2m$ is already first order, we need only keep leading order terms in the wave functions to find the non-relativistic form factor. It is clear that to leading order: $\psi(x, \mathbf{p}^\perp) \rightarrow \psi(\mathbf{p})$, where the latter is the non-relativistic wave function. Quite similarly, we see

$$\psi(x, \mathbf{p}^\perp + (1-x) \mathbf{q}^\perp) \rightarrow \frac{1}{\alpha^2 + \mathbf{p}^2 + \mathbf{p}^\perp \cdot \mathbf{q}^\perp + \mathbf{q}^{\perp 2}/4} (\delta_a^\alpha - \delta_b^\alpha).$$

Returning to the expression for the form factor, the non-relativistic limit is then

$$F(Q^2) \rightarrow \int d\mathbf{p} \, \psi^*(\mathbf{p} + \mathbf{q}^\perp/2) \psi(\mathbf{p}). \quad (15)$$

The form factor above depends neither on the orientation of \mathbf{q}^\perp , nor of \mathbf{p} . Let us then rotate our coordinate system so that \mathbf{q}^\perp is no longer completely transverse. This three-dimensional rotation is only possible now because we are integrating $d\mathbf{p}$, which can not be done in the light-front version. Thus we have sent $\mathbf{q}^\perp \rightarrow \mathbf{q}$ while maintaining the length, $\mathbf{q}^2 = Q^2$. After this rotation, the form factor is strikingly non-relativistic and can be computed analytically using Eq. 8

$$\begin{aligned} F(Q^2)^{\text{NR}} &= \int d\mathbf{r} |\psi(\mathbf{r})|^2 e^{-i\mathbf{q} \cdot \mathbf{r}/2} \\ &= \frac{mN'}{Q} \left[\tan^{-1} \left(\frac{Q}{4a} \right) - 2 \tan^{-1} \left(\frac{Q}{2(a+b)} \right) + \tan^{-1} \left(\frac{Q}{4b} \right) \right], \end{aligned} \quad (16)$$

with N' chosen to make $F(0)^{\text{NR}} = 1$.

From this analytical result, the rms. radius can be easily calculated (see Eq. 13)

$$R_{\text{rms}} = \frac{\sqrt{a^4 + 5a^3b + 12a^2b^2 + 5ab^3 + b^4}}{2^{3/2}ab(a+b)} = 1.9395 \text{ fm.} \quad (17)$$

Comparing with our previous result, the relativistic system is larger by only 0.37%. This confirms our suspicion that relativistic effects in this deuteron model are small. We can further confirm this by looking at the difference of the relativistic form factor Eq. 11 and the non-relativistic version Eq. 16. The percent difference is plotted for low Q in Figure 2 illustrating a difference only $\sim 1\%$ in this momentum régime. The small nature of relativistic effects was noted early on [18].

5 Trouble in Asymptopia

The above plot shows the absolute percent difference continually increasing as Q increases. In this section, we investigate how the light-front form factor compares with the non-relativistic version for large Q .

5.1 Exploring Asymptopia

Given our analytic expression for the non-relativistic form factor Eq. 16, it is simple to Taylor expand about $Q = \infty$ to find its asymptotic behavior. To leading order

$$\lim_{Q \rightarrow \infty} F(Q^2) \sim \frac{64ab(a+b)^2}{Q^4} = \frac{0.080585 \text{ (GeV)}^4}{Q^4}. \quad (18)$$

The asymptotic behavior of the relativistic form factor is found with the aid of the Drell-Yan-West relation [19] (under the assumption that the end-point region dominates the form factor for large Q). This relation takes the form

$$\lim_{x \rightarrow 1} x f(x, 0) \sim (x-1)^{2\delta-1} \iff \lim_{Q \rightarrow \infty} F(Q^2) \sim (Q^2)^{-\delta}. \quad (19)$$

The x -distribution function $f(x, 0)$ can be calculated analytically using Eq. 9 with $\mathbf{q}^\perp = 0$ and subsequently expanded about $x = 1$. The leading-order term in the expansion is $\mathcal{O}[(x-1)^3]$, from which we deduce $1/Q^4$ behavior in asymptopia. Given that there were only small differences between the relativistic and non-relativistic form factors for low Q , we might expect agreement in the asymptotic region. Moreover, both form factors go as $1/Q^4$ for large Q . So when scaled by Q^4 , at worst the form factors will tend to some common difference as $Q \rightarrow \infty$.

To compare the asymptotic behavior, we have plotted the relativistic and non-relativistic form factors (scaled by Q^4) for large Q (in figure 3 we plot for experimentally relevant Q^2 , whereas in figure 4 we are mathematically contrasting the asymptotics). The non-relativistic form factor lines up well with the asymptotic limit predicted by Eq. 18. The relativistic form factor, however, markedly differs from its non-relativistic counterpart, in disagreement with the Drell-Yan-West relation Eq. 19. We remind the reader that the relativistic form factor is computed exactly for our model [20]. The huge disparity between the non-relativistic and relativistic results, shown in figure 4 warrants a complete journey through asymptopia.

5.2 Sharp Peaks at $x = 1$

Before proceeding, we note that our light front wave function Eq. 10 is properly behaved:

$$\begin{aligned} \mathbf{p}^\perp 2 \psi(x, \mathbf{p}^\perp) &\rightarrow 0 \text{ as } \mathbf{p}^\perp 2 \rightarrow \infty \text{ and} \\ \psi(x, \mathbf{p}^\perp) &\rightarrow 0 \text{ as } x \rightarrow 0, 1 \end{aligned} \quad (20)$$

These conditions stem from non-relativistic versions, and will be trivially satisfied for light-front wave functions created using Eq. 5 and 6. Thus knowing the non-relativistic wave functions are peaked for small momenta, our

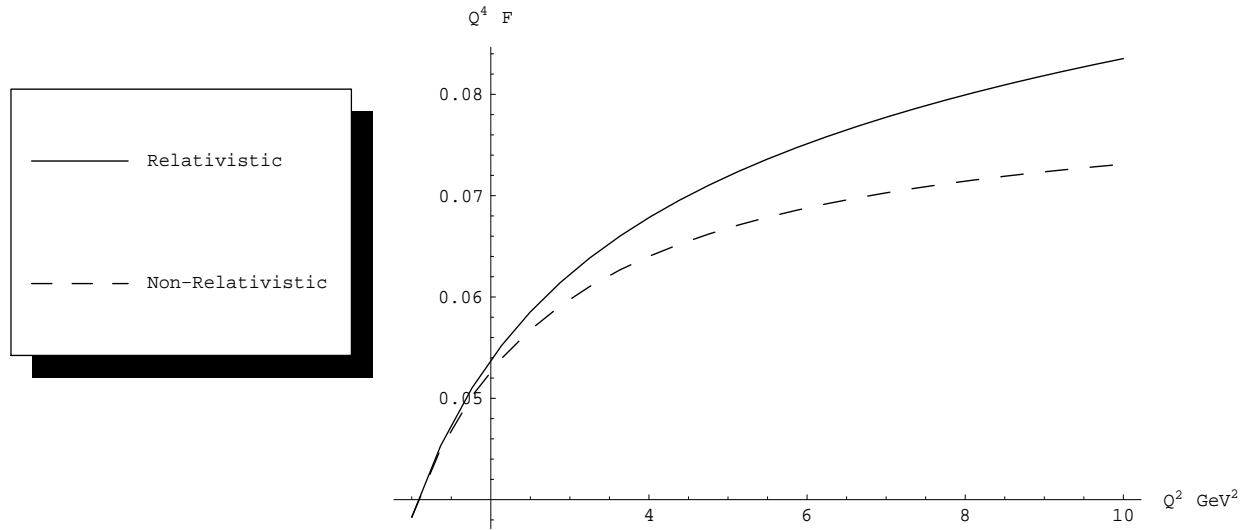


Figure 3: Relativistic and non-relativistic comparison for experimentally relevant Q^2 : the form factors are scaled by Q^4 and plotted as a function of Q^2 in GeV^2 .

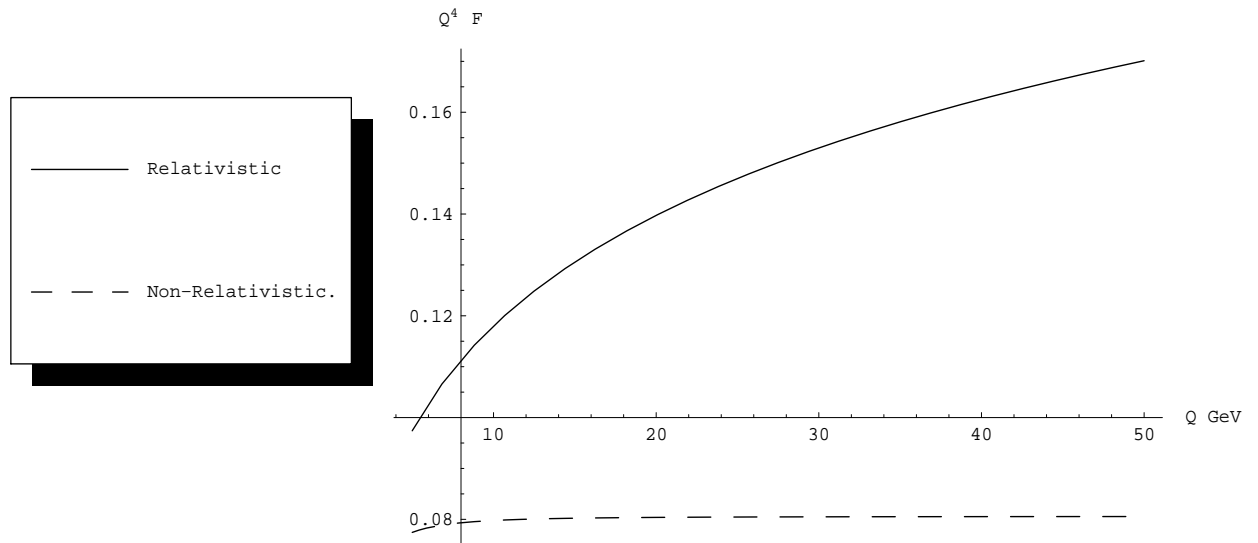


Figure 4: Relativistic and non-relativistic comparison in the asymptotic limit: the form factors are scaled by Q^4 and plotted as a function of Q in GeV .

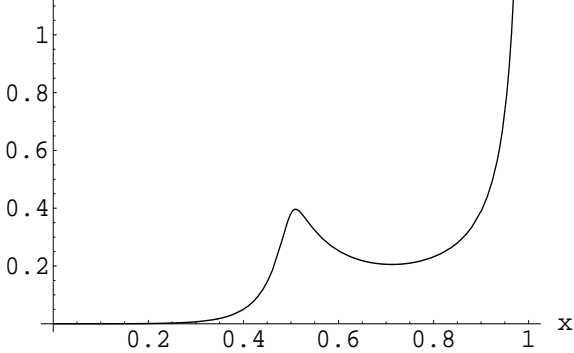


Figure 5: Plot of the integrand of Eq. 23. The singularity at $x = 1$ is too severe to bound a finite area under the curve.

light-front Hulthén wave function must be peaked for small transverse momenta. For large momentum transfer Q , Eq. 9 shows that large momentum flows through either ψ or ψ^* . Following Brodsky and Lepage [11], the dominant contributions to the form factor in the asymptotic limit come from the two regions which minimize wave function suppression

- i) $|\mathbf{p}^\perp| \ll |(1-x)\mathbf{q}^\perp|$, where $\psi^*(\mathbf{p}^\perp + (1-x)\mathbf{q}^\perp)$ is small and $\psi(\mathbf{p}^\perp)$ is large
- ii) $|\mathbf{p}^\perp + (1-x)\mathbf{q}^\perp| \ll |(1-x)\mathbf{q}^\perp|$, where $\psi(\mathbf{p}^\perp)$ is small and $\psi^*(\mathbf{p}^\perp + (1-x)\mathbf{q}^\perp)$ is large

(21)

Working first in region i, we can neglect \mathbf{p}^\perp relative to \mathbf{q}^\perp in ψ^* since the light-front wave functions are peaked for low transverse momenta. The contribution from region i is exactly the same as from ii which is made obvious by shifting \mathbf{p}^\perp . Thus dominant contributions to the form factor in the asymptotic régime appear as

$$F(Q^2) \approx 2 \int \frac{dx}{x(1-x)} \psi^*(x, (1-x)\mathbf{q}^\perp) \int d\mathbf{p}^\perp \psi(x, \mathbf{p}^\perp) \quad (22)$$

$$\approx \frac{8\pi N m^2 (b^2 - a^2)}{Q^4} \int_0^1 \frac{dx}{(1-x)^2} x^2 \log \left[\frac{4x(1-x)b^2 + (2x-1)^2 m^2}{4x(1-x)a^2 + (2x-1)^2 m^2} \right], \quad (23)$$

where we have retained the same normalization constant that appears in Eq. 12.¹ But to determine the asymptotic behavior, we must perform the integral over x which diverges! The end-point region is too peaked for the integral to converge, as illustrated by Figure 5.

The end-point region appears to dominate the form factor in asymptopia (as suggested in [21]). Perhaps the actual asymptotic behavior can be extracted by putting the end-point region under scrutiny. Above, we merely assumed the validity of the Drell-Yan-West relation; now, we will rigorously investigate it for our model.

In ascertaining the dominant contributions to the form factor in asymptopia, we have neglected the case $x = 1$. The form factor includes contributions from the end point, but this is where the scheme set up in Eq. 21 breaks down. So the above approximation Eq. 22 is really only valid for $x \leq 1 - \lambda \frac{m}{Q}$, where λ is some dimensionless cutoff

¹We obtained the same result by brute force Taylor expansion of Eq. 12 about $Q = \infty$. Since the integral over x diverges, the series expansion of $f(x, Q^2)$ lacks uniform convergence.

less than one. For $1 - \lambda \frac{m}{Q} \leq x \leq 1$, we must return to the full expression for the form factor to get the end-point contribution. To leading order, however, $(1-x) \mathbf{q}^\perp \approx \lambda m \mathbf{q}^\perp / Q$ in the end-point region and the contribution to the form factor reads

$$F(Q^2)^{\text{EP}} \approx \int_{1-\lambda \frac{m}{Q}}^1 \frac{dx}{x(1-x)} \int d\mathbf{p}^\perp \psi^*(x, \mathbf{p}^\perp + \lambda m \hat{\mathbf{q}}^\perp) \psi(x, \mathbf{p}^\perp), \quad (24)$$

where $\hat{\mathbf{q}}^\perp = \mathbf{q}^\perp / Q$ is the direction of \mathbf{q}^\perp . Since this contribution to the form factor depends only on Q^2 , we can rotate our coordinates about the z -axis to make \mathbf{q}^\perp parallel to \hat{x} . The resulting functional form is entirely similar to the full form factor, enabling swift evaluation:

$$F(Q^2)^{\text{EP}} = \int_{1-\lambda \frac{m}{Q}}^1 f(x, \lambda^2 m^2) dx \quad (25)$$

with $f(x, k^2)$ given by Eq. 12. The leading-order contribution to the above integral in asymptopia is found by expanding the integrand about $x = 1$ and integrating. The result is

$$F(Q^2)^{\text{EP}} = 8\pi N(b^2 - a^2)^2 \frac{\lambda^6 + 2\lambda^4 - 8\lambda^2 - 2\lambda(\lambda^2 + 1)\sqrt{\lambda^2 + 4}}{Q^4(\lambda^2 + 1)^3} \log \left[\frac{\sqrt{\lambda^2 + 4} - \lambda}{\lambda^3 + 3\lambda + (\lambda^2 + 1)\sqrt{\lambda^2 + 4}} \right] \quad (26)$$

which agrees with the Drell-Yan-West relation. To quantitatively consider the contribution from the end-point region, we have plotted the percent contribution to the form factor from $0 \leq x \leq 1 - \lambda \frac{m}{Q}$. We have chosen the value of λ to be smaller than one. Figure 6 shows that the bulk of the form factor does not come from the end-point region.

5.3 Divide and Conquer

In the process of trying to deduce the asymptotic behavior, our model has become infinitely sensitive to the end-point region. From the exact Hulthén form factor Eq. 11, however, we know the end-point region does not overwhelmingly contribute (as Figure 6 confirms). Our dilemma sounds familiar [22] and our approach, not surprisingly, is a regularization cutoff.

To start, let us just toss away the troublesome divergent part of Eq. 22 by introducing the cutoff λ into the x integral

$$F(Q^2) \rightarrow 2 \int_0^{1-\lambda \frac{m}{Q}} \frac{dx}{x(1-x)} \psi^*(x, (1-x) \mathbf{q}^\perp) \int d\mathbf{p}^\perp \psi(x, \mathbf{p}^\perp). \quad (27)$$

The cutoff integral above can be computed analytically. Using the integrand of Eq. 23, the result reads

$$\lim_{Q \rightarrow \infty} F(Q^2) \sim \frac{32\pi N(b^2 - a^2)^2}{Q^4} \left[\chi(a, b, m) - \log \lambda + \log \frac{Q}{m} \right], \quad (28)$$

where $\chi(a, b, m)$ is a rather complicated, page-long function independent of λ . For our parameters a, b and m , we have $\chi = 1.3635$. Nonetheless, we have discovered behavior via regularization which differs from $1/Q^4$ in a model which knows nothing about ultraviolet divergences, renormalization, etc.

One would think that with Eq. 28, we have determined the asymptotic behavior of the form factor. Although we threw away the end-point region to arrive at the above expression, we know precisely its contribution for a given λ , *cf* Eq. 26. The question remains: have we found all contributions to $\mathcal{O}[1/Q^4]$?

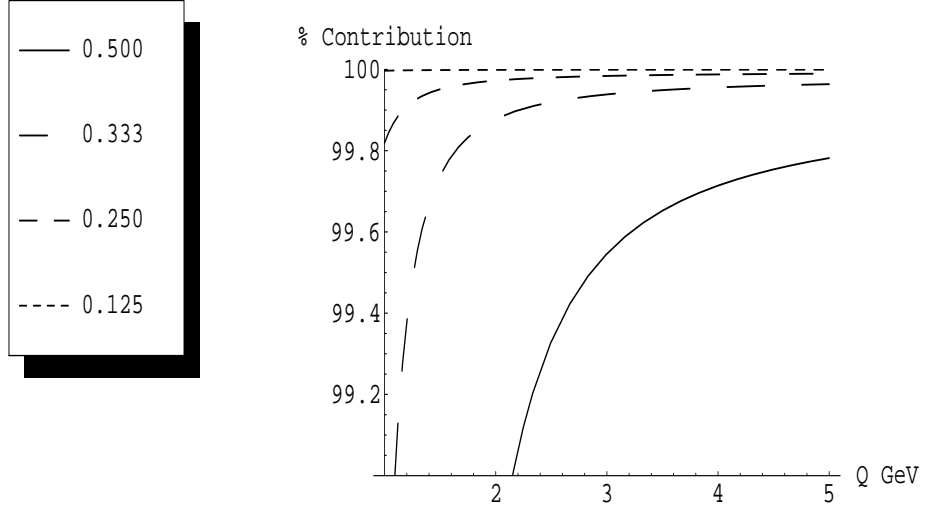


Figure 6: Percent contribution to the form factor (Eq. 11) from the region $0 \leq x \leq 1 - \lambda \frac{m}{Q}$ as a function of Q in GeV for different λ . As indicated, the end-point region is *not* dominant for asymptotic Q .

There are order $1/Q^6$ corrections to the integrand of equation 23. Putting these in give a correction term:

$$\frac{-16\pi m^2 N(b^2 - a^2)}{Q^6} \int_0^{1-\lambda \frac{m}{Q}} \frac{dx}{(1-x)^4} \frac{x^2}{(2x-1)^2} \left[2x(1-x)(a^2 + b^2) + (2x-1)^2 m^2 \right] \log \left[\frac{4x(1-x)b^2 + (2x-1)^2 m^2}{4x(1-x)a^2 + (2x-1)^2 m^2} \right]$$

Evaluating this correction term to leading order gives: $\frac{-32\pi N(b^2 - a^2)^2}{Q^4 \lambda^2}$. Thus terms in the integrand of order $1/Q^6$ give a contribution of order $1/Q^4$ to the asymptotic form factor. We haven't exhausted all of the $1/Q^6$ corrections, however—we originally took only the first term in the Taylor expansion of Eq. 9 about $\mathbf{p}^\perp = (1-x)\mathbf{q}^\perp$ and the next non-vanishing term gives contributions of order $1/Q^6$. Even if we were to collect all the $\mathcal{O}[1/Q^6]$ corrections to the x -integrand, we would have only just begun. One can easily find terms in the integrand of order $1/Q^8$ which emerge from the regularized x -integral $1/Q^4$. In fact, the integrand's correction terms of any order contribute to leading order in asymptopia!

Certainly we cannot hope to evaluate infinitely many leading-order terms. At least we have stumbled on to a prediction for the functional form in the asymptotic limit. Namely, we have seen

$$\lim_{z \rightarrow \infty} z^4 F(z^2) = \alpha + \beta \log z, \quad (29)$$

with $z \equiv Q/m$. We can test this prediction against the actual form factor's asymptotic limit calculated from equation 11. In figure 7, we test this hypothesis for empirically determined coefficients $\alpha = 0.039472$ and $\beta = 0.044930$ (calculated for z around 400). As the figure shows, this is indeed the form factor's behavior in asymptopia. It is quite curious to note: using Eq. 28, we would predict $\beta = 0.045020$ a difference of only 0.20% when compared with the empirical value. We believe this discrepancy results from approximating asymptotic z as around 400, not from

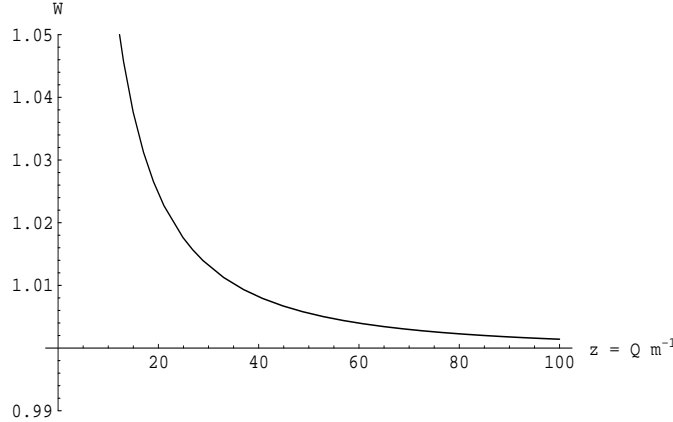


Figure 7: Asymptotic Behavior of $F(Q^2)$ given by Equation 11: $W = \frac{z^4 F(z^2) - \alpha}{\beta \log z}$ is plotted as a function of $z = \frac{Q}{m}$ for the parameters $\alpha = 0.039472$ and $\beta = 0.044930$ which were graphically determined for z around 400.

ignoring infinitely many leading-order corrections. Indeed, we never found corrections of order $\log z/z^4$ above, only a myriad of $1/z^4$ terms. It is our belief that the coefficient β can be ascertained from the regularization integral Eq. 28. The leading correction² to β determined graphically is $\mathcal{O}[1/z^5]$ —which gives a relative correction of 0.25% for $z \sim 400$. Taking z larger in order to reduce this term only results in appreciable error in numerical integration. To verify our conjecture, we have attempted to find the coefficient β by varying z . Figure 8 shows a plot of the graphically found value of β as a function of z (the midpoint of our interval). Specifically we use a simple linear fit in the plot

$$\beta(z) = \left((z+50)^4 F(z+50) - (z-50)^4 F(z-50) \right) \log \left[\frac{z-50}{z+50} \right]. \quad (30)$$

The plot shows our cited value $\beta = 0.044930$ at $z = 400$. The trend is clear, β is increasing to some limiting value as z increases. The numerical integration, however, becomes unreliable to $\sim 1\%$ past 600. Nonetheless, it appears we can determine β from the regularization integral 28. We are at a loss, however, to predict α : there are simply an infinite number of correction terms to $\mathcal{O}[1/Q^4]$ to evaluate.

6 Similar Problems

The problems encountered above are not unique to the Huthén model. In this section, we begin by exploring another model with similar behavior in asymptopia.

²Expanding the integrand of the form-factor in powers of Q , there are only even terms. Once we exit the cutoff integral, however, we can now have any power of Q in the expansion.

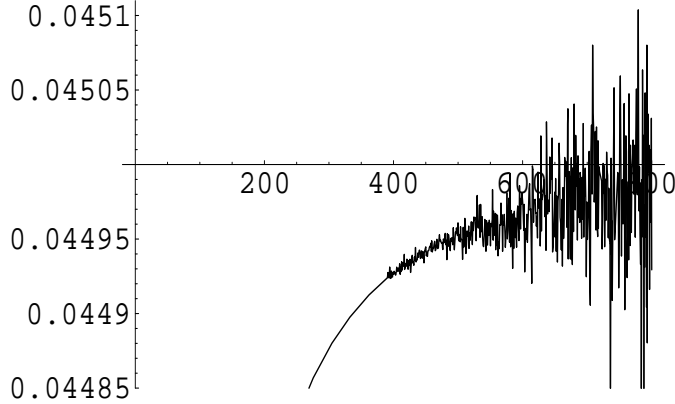


Figure 8: Simple numerical determination of β (via Equation 30) plotted as a function $z = \frac{Q}{m}$. The numerical integration clearly becomes imprecise past $z = 600$.

6.1 Coulomb Potential

Let us suppose our particles interact via a Coulomb potential $V(r) \sim 1/r$, for which we take $\psi(\mathbf{r}) = e^{-\kappa r}$. Then our momentum-space solution to Eq. 6 is given by

$$\begin{aligned} \psi(x, \mathbf{p}^\perp) &\equiv \frac{m^3 \sqrt{N}}{16(\kappa^2 + \mathbf{p}^2)^2} \\ &= \frac{m^3 \sqrt{N} x^2 (1-x)^2}{(4x(1-x)\kappa^2 + \mathbf{p}^\perp{}^2 + (2x-1)^2 m^2)^2}, \end{aligned} \quad (31)$$

where we have used Eq. 5 to re-express p^3 in the light-front center of mass. To find the asymptotic behavior of this model's form factor, we use Eq. 22. Performing the integration, leaves us with a logarithmically divergent x -integral:

$$\lim_{Q \rightarrow \infty} F(Q^2) = \frac{m^6 N \pi}{Q^4} \int_0^1 \frac{dx}{(1-x)[4x(1-x)\kappa^2 + (2x-1)^2 m^2]} x^3. \quad (32)$$

Restricting x to the range $0 \leq x \leq 1 - \lambda \frac{m}{Q}$, and performing the integral yields

$$\lim_{Q \rightarrow \infty} F(Q^2) = \frac{m^4 N \pi}{Q^4} \left[\chi(\kappa, m) - \log \lambda + \log \frac{Q}{m} \right]. \quad (33)$$

6.2 Why Regularization?

As we have seen above, determining the exact asymptotic behavior of light-front form factors is no trivial task. The Drell-Yan-West relation is still apt at describing the contribution from the end-point region, however, this region does not dominate our form factors for asymptotic Q . Furthermore, techniques to determine the asymptotic

behavior (brute force Taylor expansion, finding contributions from regions of minimal wave function suppression) led to logarithmically divergent x -integrals, suggesting the non-commutativity of the limits: $Q \rightarrow \infty$ and $x \rightarrow 1$. Here we show how the potentials we use cause the peculiarities for $x \rightarrow 1$.

Starting with the expression for the light-front form factor Eq. 9, we were led to the dominant contribution in asymptopia via isolating the regions of minimal wave function suppression, namely

$$\lim_{Q \rightarrow \infty} F(Q^2) \approx 2 \int \frac{dx}{x(1-x)} \psi(x, (1-x) \mathbf{q}^\perp) \int d\mathbf{p}^\perp \psi(x, \mathbf{p}^\perp).$$

Now let us utilize the Weinberg equation [13], which is the momentum-space version of our Eq. 4:

$$\psi(x, \mathbf{p}^\perp) = \frac{m^2/2\pi^3}{M^2 - \frac{\mathbf{p}^{\perp 2} + m^2}{x(1-x)}} \int \frac{dy}{y(1-y)} d\mathbf{k}^\perp \psi(y, \mathbf{k}^\perp) V(x, \mathbf{p}^\perp; y, \mathbf{k}^\perp), \quad (34)$$

with V as the Fourier transform of the potential. We can use this information in the asymptotic limit of the form factor, namely for

$$\psi(x, (1-x) \mathbf{q}^\perp) \approx -\frac{m^2 x}{2\pi^3 (1-x) Q^2} \int \frac{dy}{y(1-y)} d\mathbf{k}^\perp \psi(y, \mathbf{k}^\perp) V(x, (1-x) \mathbf{q}^\perp; y, \mathbf{k}^\perp) \quad (35)$$

Of course, in asymptopia the integral containing V can be simplified. The potentials considered above are of the form $V = V(|\mathbf{p} - \mathbf{k}|)$, where

$$(\mathbf{p} - \mathbf{k})^2 = \left(\mathbf{p}^\perp - \mathbf{k}^\perp \right)^2 + \left((x-1/2) \sqrt{\frac{\mathbf{p}^{\perp 2} + m^2}{x(1-x)}} - (y-1/2) \sqrt{\frac{\mathbf{k}^{\perp 2} + m^2}{y(1-y)}} \right)^2 \quad (36)$$

which makes explicit use of having two equally massive particles in the center of mass frame (*cf* Eq. 5). As a result of the above equation, $V(x, (1-x) \mathbf{q}^\perp; y, \mathbf{k}^\perp) = V(x, (1-x) \mathbf{q}^\perp; 1/2, 0)$ to leading order. Henceforth we shall abbreviate $V(x, (1-x) \mathbf{q}^\perp; 1/2, 0) = V(|\mathbf{q}(x)|)$, where

$$|\mathbf{q}(x)| = \sqrt{(1-x)^2 Q^2 + (q^3)^2} = \frac{Q}{2} \sqrt{\frac{1-x}{x}} \quad (37)$$

Revising the expression for the asymptotic form factor, we find (neglecting overall constants)

$$\lim_{Q \rightarrow \infty} F(Q^2) \sim \int \frac{dx \phi(x)}{(1-x)^2 Q^2} V(|\mathbf{q}(x)|), \quad (38)$$

where $\phi(x) = \int d\mathbf{p}^\perp \psi(x, \mathbf{p}^\perp)$ and the y -dependence integrated itself away. Eq. 38 contains the answer to our troubled journey through asymptopia. At first glance, the integrand appears singular at the end point: containing one factor of $1-x$ from the measure, and another from the $(1-x) \mathbf{q}^\perp$ contained in the form factor. These factors are quite general and contain nothing specific about the interaction. While Eq. 20 spells out the criteria for good wave functions, it is necessary to be further restrictive by requiring $\psi(x, \mathbf{p}^\perp) \sim (1-x)^2$ as $x \rightarrow 1$ if we wish to cancel the potentially singular denominator in Eq. 38. This isn't much of an imposition; both the Hulthén wave function Eq. 10 and the Coulomb wave function Eq. 31 go like $(1-x)^2$ as $x \rightarrow 1$!

Only one x -dependent piece of Eq. 38 remains to be considered—the potential. It is now immediately obvious that the Coulombic form factor should suffer logarithmic divergences in asymptopia:

$$V^C(|\mathbf{q}(x)|) \sim -\frac{1}{\mathbf{q}(x)^2} = -\frac{4x}{(1-x)Q^2}. \quad (39)$$

The potential brings along the anticipated factor of Q^2 , but on the light front, an unwanted $(1-x)$ tags along. Given the behavior of the light front wave function, this extra factor is just enough to make the integral in Eq. 38 diverge. The same is true for the Hulthén potential Eq. 7, since we have

$$\lim_{Q \rightarrow \infty} V^H(|\mathbf{q}(x)|) = -\frac{12\pi(a+b)}{\mathbf{q}(x)^2} = -\frac{48\pi(a+b)x}{(1-x)Q^2}. \quad (40)$$

As illustrated above (Figures 1-4), the form factor itself isn't singular at asymptotic Q , just our means of obtaining it. This is made obvious by commuting the limits. Above we looked at $Q \rightarrow \infty$ first and found problematic behavior for $x \rightarrow 1$ stemming from the potential. On the other hand, consider taking x near one first. We already did this for the Hulthén form factor, see Eq. 24. Now we are in a position to generalize this result. Since we know our wave functions $\psi(x, \mathbf{p}^\perp) \sim (1-x)^2$ as $x \rightarrow 1$, the contribution from the end point becomes:

$$F(Q^2)^{\text{EP}} \sim \int_{1-\lambda \frac{m}{Q}}^1 (1-x)^3 dx \rightarrow \frac{1}{Q^4}.$$

This is just the Drell-Yan-West relation, which, as we have seen, does not account for the majority of the form factor in asymptopia. Clearly different behavior is seen when looking at asymptotic Q near the end point, versus the end-point region for asymptotic Q !

Logarithmically divergent form factors in asymptopia need not plague us any longer. The culprit has been unmasked: potentials in the *auxiliary* coordinate-space, such as the $1/r$ of the Coulomb model or Eq. 7 for the Hulthén, which are $\sim 1/r$ for small r will lead to logarithmic divergences in the expression for the asymptotic form factor. Of course, the asymptotic form factor *itself* is not singular. The logarithmic divergence of our asymptotic expression is a thorn-like warning: the series expansion in $1/Q$ does not converge uniformly in x .

6.3 Realistic Models on the Light Front

Above we have seen rather simplistic models lead to electromagnetic form factors with non-standard asymptotic behavior. It is not likely, however, that this behavior is physical—though certainly it is the true asymptotic behavior for the models considered.

Early work on factorization in quantum chromodynamics showed similar logarithms appearing in asymptopia [23] for the nucleon electric form factor, and thus a failure of renormalization group techniques. Quite soon there after, it was realized [24] that these logarithms were just manifestations of neglected higher-order corrections. Apparent end-point singularities are removed when evolution of the longitudinal momentum amplitude ϕ is properly included, and consequently factorization is saved [25].

Obviously our models do not have such higher-order corrections, and thus the logarithm remains. We must then wonder whether factorization breaks down for more realistic models on the light front. Let us then consider a more sophisticated model of the deuteron arising from meson-theoretic potentials [26]. The general parameterization of the s-wave deuteron wave function is

$$\psi(r) = \frac{1}{r} \sum_{j=1}^N C_j e^{-m_j r} \quad (41)$$

with

$$m_j = \alpha + (j-1)m_o.$$

The usual boundary condition (finite wave function at the origin) leads to the constraint

$$\sum_{j=1}^N C_j = 0. \quad (42)$$

To put this realistic deuteron model on the light front, we work in momentum space and use the longitudinal momentum prescription above (Eq. 5). The resulting form factor is completely similar to that of the Hulthén (Eq. 11) except there are now N^2 terms instead of 4. At this point, the similarity leads us to suspect Q^4 behavior modified by a logarithm in asymptopia. Based on our above analysis, verification of the logarithm's presence requires that we check $\psi(x, \mathbf{p}^\perp) \sim (1-x)^2$ as $x \rightarrow 1$ and that the potential in r -space goes like $1/r$ near the origin.

The momentum-space wave function has the end-point behavior

$$\psi(x, \mathbf{p}^\perp) \sim \sum_{j=1}^N C_j m_j^2 \frac{(1-x)^2}{(m^2 + \mathbf{p}^\perp)^2} + \mathcal{O}[(1-x)^3], \quad (43)$$

where the term linear in $1-x$ has vanished due to the constraint equation 42. Appealing to the wave equation 6, we can determine the potential which generates this deuteron wave function

$$V^{\text{MT}}(r) = \frac{\sum_{j=1}^N C_j [2(\alpha - m_o)m_o j + m_o^2 j^2] e^{-m_o r j}}{\sum_{\ell=1}^N C_\ell e^{-m_o r \ell}} + \text{const}, \quad (44)$$

where the constant ensures the potential vanishes as $r \rightarrow \infty$. It is then straight forward to find the behavior near the origin

$$\lim_{r \rightarrow 0} V^{\text{MT}}(r) = -\frac{1}{r} \left[2(\alpha - m_o) + m_o \frac{\ell(N)}{k(N)} \right], \quad (45)$$

where $\ell(N) = \sum j C_j$ and $k(N) = \sum j^2 C_j$. Thus based on these analytic observations, equation 38 shows that even a realistic deuteron model will be troublesome in asymptopia.

7 Conquering Asymptopia

As we have seen, equation 38 is a rather naïve way to determine a form factor's asymptotic behavior. This equation and the analysis leading to it were extrapolated from our knowledge of non-relativistic wave functions. Indeed one may verify that equation 22 (derived by an analysis parallel to the non-relativistic one [11]) gives exactly the same results as equation 38. The breakdown of factorization for the above models is clearly a *relativistic* problem (further verified by equation 37). Equation 38 may not be useful in determining the asymptotic behavior. Without it, however, we wouldn't be aware of the cause of our problems at high momentum transfer. Now knowing when to expect trouble in asymptopia, let us proceed to correctly deduce the asymptotic behavior.

7.1 Wick-Cutkosky Model

Before returning to the asymptotics of the Hulthén form factor, let us take a worthwhile look at the Wick-Cutkosky model. Consider two equally massive scalar particles which interact by exchanging a massless scalar particle. The

potential for such a process has been found and consequently the ground-state wave function can be deduced using the momentum-space version of equation 6. The wave function is [27]

$$\begin{aligned}\psi(x, \mathbf{p}^\perp) &= \frac{8\sqrt{\pi}\kappa^{5/2}}{(\mathbf{p}^2 + \kappa^2)^2 \left(1 + \left|\frac{p^3}{E(\mathbf{p})}\right|\right)} \\ &= \frac{2^7 \sqrt{\pi} \kappa^{5/2} x^2 (1-x)^2}{(4x(1-x)\kappa^2 + \mathbf{p}^\perp{}^2 + (2x-1)^2 m^2)^2 (1 + |2x-1|)},\end{aligned}\quad (46)$$

where we have used the energy $E(\mathbf{p}) = \frac{1}{2}\sqrt{\frac{\mathbf{p}^\perp{}^2 + m^2}{x(1-x)}}$ in the two-particle center of mass, and p^3 is given by equation 5. Here $\kappa = \frac{1}{2}ma$ and $a = g^2/16\pi m^2$ with g as the coupling constant present in the interaction term. The invariant mass of the system is $M = 2m - \frac{1}{4}ma^2$. To write this wave function, we have converted the explicitly covariant form cited in [27] into our own z -axis dependent form. The difference between these approaches does not concern us for the ground state of scalar particles. For a review of explicitly covariant light-front dynamics see [28] or [29]. The wave function in equation 46 is quite similar to our Coulomb wave function in section 6.1. The extra term in the denominator originates from retardation effects contained in the relativistic potential (effects which our naïve models clearly lack). The behavior of the wave function at the end point is not modified (to leading order in $1-x$) by retardation. Furthermore, the retarded potential is [27]

$$V(x, \mathbf{p}^\perp; y, \mathbf{k}^\perp)^{\text{WC}} = -4\pi a/\mathcal{K}^2, \quad (47)$$

with

$$\mathcal{K}^2 = (\mathbf{p} - \mathbf{k})^2 - (2x-1)(2y-1)(E(\mathbf{p}) - E(\mathbf{k}))^2 + 2|x-y|\left(E(\mathbf{p})^2 + E(\mathbf{k})^2 - \frac{M^2}{2}\right),$$

where $(\mathbf{p} - \mathbf{k})^2$ is given by equation 36. Using this potential for asymptotic Q , we note

$$V(x, (1-x) \mathbf{q}^\perp; 1/2, 0)^{\text{WC}} \approx -\frac{16\pi a x}{(1-x)Q^2(1+|2x-1|)} \quad (48)$$

which is singular at $x = 1$. Given this and the wave function's end-point behavior, we once again appeal to equation 38 and a logarithmically divergent x -integral confronts us in deducing the asymptotic behavior of the form factor. Our experience above leads us to believe the true asymptotic behavior is Q^{-4} modified by a logarithm. This asymptotic behavior for the Wick-Cutkosky model has been found previously by Karmanov and Smirnov [9] by considering regions which dominate the x and \mathbf{p}^\perp integrals of the form factor. The same asymptotic behavior of the Wick-Cutkosky model was also found [9] by using the Bethe-Salpeter approach. Karmanov and Smirnov state that the logarithmic $\log Q^2/Q^4$ behavior was also been found earlier in [30]—a paper which admits the possibility of such logarithms only by announcing it is not considering such cases. Nonetheless, the correct asymptotic behavior of the Wick-Cutkosky form factor was deduced in [9] as we shall now demonstrate using techniques considered above.

Considering the analytic form of the wave function 46, we can see a region which dominates the form factor for asymptotic Q : x near $\frac{1}{2}$. In this case, we can surely say $(1-x)Q \approx \frac{Q}{2} \gg m$ and consequently the analysis leading to equation 22 is certainly valid. Moreover, the Wick-Cutkosky wave function is identical to our Coulomb wave function for $x \approx \frac{1}{2}$. Thus appealing to equation 22, we find (to leading order about $x = \frac{1}{2}$)

$$\begin{aligned}\lim_{Q \rightarrow \infty} F(Q^2) &= \frac{16m^4 a^5}{\pi Q^4} \int_0^1 \frac{dx}{\frac{a^2}{4} + (2x-1)^2} \\ &= \frac{16m^4 a^4}{Q^4} (1 + \mathcal{O}[a]),\end{aligned}\quad (49)$$

where we have assumed $a \ll 1$ so that $x(1-x)a^2 \approx a^2/4$. In order to compare with [9], we have been careful to adopt their normalization (we have multiplied our expression 9 by $\frac{m}{2}(2\pi)^{-3}$.)

The other dominant contribution in asymptopia comes from *near* the end-point region $\frac{1}{2} < (1-x) \ll 1 - \lambda \frac{m}{Q}$ as we have seen above by producing logarithms from regularized x -integrals. We can thus deduce the remaining contribution in asymptopia via regularization. This result will be different from the Coulomb result, equation 33, due to the retardation factor. First we note that in the near end-point region $x(1-x)a^2 \approx 0$. Now take $\frac{1}{2} < x_o < 1 - \lambda \frac{m}{Q}$ and hence the contribution which interests us reads

$$\begin{aligned} \lim_{Q \rightarrow \infty} F_\lambda(Q^2) &\equiv \frac{64m^4a^5}{\pi Q^4} \int_{x_o}^{1-\lambda \frac{m}{Q}} \frac{x \, dx}{4(1-x)(2x-1)^2} \\ &= \frac{16m^4a^5}{\pi Q^4} \left[\xi(x_o, a, m) - \log \lambda + \log \frac{Q}{m} \right] \left(1 + \mathcal{O}\left[\frac{1}{Q}\right] \right) \end{aligned} \quad (50)$$

Combining these two results (using only the logarithmic part of the latter), we arrive at the asymptotic behavior (to leading order in a)

$$\lim_{Q \rightarrow \infty} F(Q^2) \approx \frac{16m^4a^5}{\pi Q^4} \left(\log \frac{Q}{m} + \frac{\pi}{a} \right) \quad (51)$$

which agrees with the result found by Karmanov and Smirnov [9]. Furthermore one can use the Wick-Cutkosky wave function above to numerically calculate the form factor and test equation 51 as predicting its asymptotic behavior. This form factor is less complicated than the Hulthén model's. Consequently, the numerical integration is precise to larger Q . As before, we have graphically determined the coefficients α, β in equation 29 and observed the asymptotic behavior as tending toward $(\alpha + \beta \log z)/z^4$, with $z = \frac{Q}{m}$. The coefficient β agrees well with equation 51, differing by $< 0.1\%$ for $a = 0.08, 0.007$. The error of the coefficient α depends on how rapidly the series in a converges. For $a = 0.08$, our graphically determined α differs from equation 51 by $\sim 12\%$. While for $a = 0.007$, the error is $\sim 2\%$. Indeed we have deduced the form factor's asymptotic behavior.

7.2 Back to the Hulthén

Our analysis above has been quite general and we shall now apply it to the Hulthén form factor. To finish our quest through asymptopia, it remains to determine the coefficient α in equation 29 for the Hulthén model. As we learned above³, considering the contribution for $x \approx \frac{1}{2}$ gives us α for asymptotic Q . So we return to equation 23 and expand to leading order about $x = \frac{1}{2}$

$$\lim_{Q \rightarrow \infty} F(Q^2) \approx \frac{4\pi m^2 N(b^2 - a^2)}{Q^4} \int_0^1 \log \left[\frac{b^2 + (2x-1)^2 m^2}{a^2 + (2x-1)^2 m^2} \right] dx. \quad (52)$$

having used $\frac{a}{m}, \frac{b}{m} \ll 1$. At first glance, it appears we have dropped a factor of two from the asymptotic expression 23. However careful consideration of region i (in equation 21), shows its contribution vanishes (to leading order in $1/Q$). Evaluating the above integral and combining with the logarithmic part of our previous result (equation 28), we find

$$\lim_{Q \rightarrow \infty} F(Q^2) = \frac{32\pi N(b^2 - a^2)^2}{Q^4} \left[\log \frac{Q}{m} + \frac{1}{8} \left(\frac{m\pi}{b+a} - 1 \right) \right]. \quad (53)$$

³ A more precise statement is: expanding about $x = \frac{1}{2}$ in equation 22 gives the coefficient α up to a possible factor of 2.

From which we deduce $\alpha = 0.046493$ (and $\beta = 0.045020$ as discussed previously). Comparing with the graphically determined result of section 5.3, we see that there is a 17.8% difference. Again this difference is due to the series expansion in small parameters: $a/m = 0.048943$ and $b/m = 0.29007$. For smaller values of the parameters, we expect better results. However, with smaller parameters one needs higher Q to graphically determine α, β and the numerical integration becomes imprecise. Nonetheless, within our constraints we have verified equation 53 as the asymptotic behavior of the Hulthén form factor.

8 Concluding Remarks

We have undertaken a relatively simple task to compare relativistic and non-relativistic form factors for the Hulthén model of the deuteron. For small momentum transfer, the two versions differ by about a percent and the root mean square radii differ by even less. The behavior for large Q , however, led us on an unexpected journey.

Our expedition through asymptopia helped us learn the Hulthén form factor's true behavior $\sim \log Q^2/Q^4$ for large Q . The path was circuitous because the conventional means (asymptotic expressions, Taylor series expansions) lead directly to logarithmic divergences. These difficulties are manifestations of the non-commutativity of the limits $Q \rightarrow \infty$ and $x \rightarrow 1$, and hence indicative of the breakdown of factorization.

Indeed, we find that this behavior is not particular to the Hulthén model. Equation 38 tracks down the root of these difficulties. Generating our light front wave functions from non-relativistic potentials singular at the origin will lead to problematic relativistic form factors in the asymptotic limit. Such problems do not plague calculations in fundamental theories because higher-order corrections necessarily cancel the divergences. For realistic models, however, the breakdown of factorization persists and is an obstruction to straightforward asymptotic calculations.

Acknowledgment

This work was funded by the U. S. Department of Energy, grant: DE-FG03 – 97ER41014.

References

- [1] P. A. M. Dirac, Rev. Mod. Phys. **21** (1949) 392.
- [2] D. E. Soper, *Field Theories in the Infinite Momentum Frame*, SLAC pub-137 (1971); D. E. Soper, Phys. Rev. **D4** (1971) 1620; J. B. Kogut and D. E. Soper, Phys. Rev. **D1** (1971) 2901.
- [3] S-J. Chang, R. G. Root, and T-M. Yan, Phys. Rev. **D7** (1973) 1133, 1147.
- [4] T-M. Yan, Phys. Rev. **D7** (1974) 1706, 1708.
- [5] L. L. Frankfurt and M. I. Strikman, Phys. Rep. **76** (1981) 215.
- [6] P. G. Blunden, M. Burkardt, and G. A. Miller, Phys. Rev. **C61** (2000) 025206.
- [7] G. A. Miller, Prog. Part. Nuc. Phys **45** (2000) 83.
- [8] G. G. Petratos, Nucl. Phys. **A663** (2000) 357.
- [9] V. A. Karmanov and A. V. Smirnov, Nucl. Phys. **A546** (1992) 691.
- [10] A. Harindranath, *An Introduction to Light Front Dynamics for Pedestrians*, hep-ph/9612244.

[11] S. J. Brodsky and G. P. Lepage, *Exclusive Processes in Quantum Chromodynamics*, in **Perturbative Quantum Chromodynamics**, A. H. Mueller ed., World Scientific Publishing, 1989.

[12] M. V. Terent'ev, Sov. J. Nucl. Phys. **24** (1976) 106.

[13] S. Weinberg, Phys. Rev. **150** (1966) 1313.

[14] Starting with a two body light-front Hamiltonian $P^- \psi = \left(\frac{\mathbf{k}_1^{\perp 2} + m^2}{\mathbf{k}_1^+} + \frac{\mathbf{k}_2^{\perp 2} + m^2}{\mathbf{k}_2^+} + \mathcal{V} \right) \psi$ and repeating the above algebra in the center of mass frame, we see that $V^H = M\mathcal{V}/4$.

[15] M. G. Fuda, Phys. Rev. **D41** (1990) 534; Phys. Rev. **D42** (1990) 2898; Phys. Rev. **D44** (1991) 1880.

[16] C. W. Wong, Int. J. Mod. Phys. **E3** (1994) 821.

[17] J. F. Gunion, S. J. Brodsky, and R. Blankenbecler, Phys. Rev. **D8** (1973) 287.

[18] L. L. Frankfurt and M. I. Strikman, Nucl. Phys. **B148** (1979) 107.

[19] S. D. Drell and T-M. Yan, Phys. Rev. Lett. **24** (1970) 181; G. West, Phys. Rev. Lett. **24** (1970) 1206.

[20] There are small errors in numerical integration, however. They amount to only one part in 10^{10} for the range of Q plotted in Figure 4. We must go to higher Q for the error to accumulate to $\sim 1\%$, see Figure 8.

[21] R. P. Feynman, **Photon-Hadron Interactions**, W. A. Benjamin, Reading, Massachusetts, 1972.

[22] G. P. Lepage, *How to Renormalize the Schrödinger Equation*, Lectures at the VIII Jorge André Swieca Summer School, Brazil, 1997, nucl-th/9706029.

[23] A. Duncan and A. H. Mueller, Phys. Rev. **D21** (1980) 1636.

[24] G. P. Lepage and S. J. Brodsky, Phys. Rev. **D22** (1980) 2157.

[25] It is curious to note that the functional forms involved for the light front Hulthén model are remarkably similar to end-point region suppression via Sudakov form factors due to gluon corrections to the quark-photon vertex (see Appendix E of [24]) with the exception that our transverse integrals are finite.

[26] R. Machleidt, Adv. Nucl. Phys. **19** (1989) 189.

[27] V. A. Karmanov, Nucl. Phys. **B166** (1980) 378.

[28] J. Carbonell, B. Desplanques, V. A. Karmanov and J-F. Mathiot, Phys. Rept. **300** (1998) 215.

[29] V. A. Karmanov, *Light-Front Dynamics*, nucl-th/9907037.

[30] C. Alabiso and G. Schierholz, Phys. Rev. **D10** (1974) 960.